ORIGINAL PAPER

Influences of synthesis route and preparation process on the electrochemical properties of Fe-doped strontium cobaltite

Xiaodong Zhu · Xinbing Chen · Yixing Yuan ·
Kening Sun · Naiqing Zhang

Abstract $SrCo_{0.8}Fe_{0.2}O_{3-\delta}$ (SCF), as a promising cathode material for intermediate temperature solid oxide fuel cells, possesses a high catalytic activity for the reduction of O_2 to $2O^{2-}$. The SCF powder was successfully synthesized by the solid state reaction method and Pechini method and characterized using XRD, particle analysis, and electrochemical performance measurements. Smaller-particle-size SCF materials (SCF-P) with single phase are obtained at lower synthesis temperature by the Pechini method and possess better electrochemical performance as compared with those prepared by the solid state reaction method. The reason is that the Pechini method involves the mixing of elements at atomic level, so pure SCF phase formation can be accelerated and showed high electrocatalytic activity. The preparation procedure of SCF cathode was firstly investigated using electrochemical impedance spectroscopy. Results show that the total polarization resistance and the low-frequency resistance decrease gradually with the reduction of the calcination temperature for the SCF cathodes. The SCF-P cathode sintered at 1,000 °C possesses the highest porosity and the best electrochemical performance. It is the result of a comprehensive function of three-phase boundary length, porosity of cathode, and the adhesion between cathode and electrolyte. The charge-transfer process, together with the adsorption, dissociation, and diffusion of oxygen, has a strong influence on the whole reaction process of the cathode. The influence of binder amounts on the performance of the SCF-P cathodes was also studied.

Keywords Solid oxide fuel cell · Fe-doped strontium cobaltite · Electrochemical performance · Pechini method · Solid state reaction method

X. Zhu
State Key Laboratory of Urban Water Resource and Environment,
Harbin Institute of Technology,
Harbin, Heilongjiang 150090, China

X. Zhu · K. Sun · N. Zhang
Academy of Fundamental and Interdisciplinary Sciences,
Harbin Institute of Technology,
Harbin, Heilongjiang 150080, China

X. Zhu · Y. Yuan
Center for Post-doctoral Studies of Civil Engineering,
Harbin Institute of Technology,
Harbin, Heilongjiang 150090, China

X. Zhu · X. Chen · K. Sun (✉) · N. Zhang
Department of Applied Chemistry, Harbin Institute of Technology,
Harbin, Heilongjiang 150001, China
e-mail: keningsun@yahoo.com.cn

Introduction

Solid oxide fuel cells (SOFCs) are promising energy conversion devices that can generate electric power through electrochemical reaction between an oxidant and a fuel gas [1–3]. SOFCs can provide high total efficiency when they are used in a cogeneration system and serve as clean power sources with little production of NO_x and SO_x [4]. Lowering the operating temperature of the SOFCs can significantly reduce the cost within the scope of interconnection, manifold, and sealing materials as well as greatly increases the stability and durability of cell stacks and the balance-of-plant components [5, 6]. However, a decrease of the operation temperature means a loss of power density mainly due to a considerable reduction of both ionic conductivity of the electrolyte and catalytic activity of the electrodes. To avoid ohmic loss, the thickness of the electrolyte should be reduced or alternative electrolyte materials such as La(Sr)Ga (Mg)$O_{3-\delta}$ (LSGM) are used [7–9].

At lower temperature, Sr-doped lanthanum manganite, which is used as a cathode in the conventional SOFC, shows very high interfacial resistance at the cathode–electrolyte interface [10, 11]. So, alternative electrode materials with enhanced electrode performance at lower temperatures should be achieved. From an electrochemical standpoint, a mixed electronic and oxide-ion conduction in an electrode is the most desirable property for accelerating the rate of reduction or oxidation at the electrode provided that the mixed conductors promote the surface reactions. K. Huang et al. reported $SrCo_{0.8}Fe_{0.2}O_{3-\delta}$ (SCF) as a mixed oxide-ion/electronic conductor (MIEC) produces the highest oxygen flux of all the cobalt-containing perovskites and possesses high catalytic activity for the reduction of O_2 to $2O^{2-}$ [12–14]. The electrode reactions for the mixed conducting electrodes are only restricted to the gas–solid two-phase interface; in contrast, the reactions occur at a gas–solid–solid triple-phase boundary for a solely electron-conducting electrode. The transport of oxide ions through an MIEC electrode and across the cathode/electrolyte interface has been reported to be fast enough; the dioxygen dissociation on the gas–solid surface is usually the only rate-limiting step [15, 16]. Increasing the electrode areas is the most effective way to enhance the oxygen exchange rate at the gas–solid interface [14]. Therefore, it is important to study the preparation procedure of the SCF cathode, including the synthesis route of SCF powders.

K. Huang et al. obtained SCF single-phase powder by Pechini method at 1,000 °C synthesis temperature (ST) and prepared SCF cathode at above 1,100 °C calcination temperature (CT) [14]. Lowing ST and CT is beneficial to enlarge the electrode areas. In this work, the synthesis of pure single-phase SCF powder using Pechini method at a lower ST and a successful solid state reaction method are presented. Besides, the influences of the preparation procedure (ST and binder) on the electrochemical performance for the SCF cathode are studied in detail using electrochemical impedance spectroscopy (EIS).

Experimental

Synthesis of SCF powders

Solid state reaction synthesis. Stoichiometric amounts of $SrCO_3$, Co_2O_3, and Fe_2O_3 were ball milled for 6 h. Then, the mixture was pressed into a pellet under 35 MPa and calcined at 1,100 °C for 4 h. The process was repeated three times, and the pellet was finally sintered at 1,250 °C or 1,300 °C for 6 h to obtain the SCF powders, denoted as SCF-S (SCF-S1250 or SCF-S1300).

Pechini synthesis. $Fe(NO_3)_3 \cdot 9H_2O$, $Sr(NO_3)_2 \cdot 6H_2O$, and $Co(NO_3)_3 \cdot 6H_2O$ were used as the starting materials.

Ethylenediaminetetra-acetic acid (EDTA) as the chelating agent was first dissolved into ammonia water to get a clear solution. Then, stoichiometric amounts of nitrates were dissolved into the ammonia solution with stirring. Excess ethylene glycol and citric acid (1.2:1) were added dropwise as the curing agents. The mole ratio of EDTA:CA:metal ions in the solution was 1.2:1.2:1. The pH of the prepared solution was adjusted to 7.5 with concentrated ammonia. The solution was heated to 100 °C and maintained at this temperature to favor the complexation process of the metal cations and the polyesterification reactions. Initially, a sol and, finally, a resin were obtained during heating. The resin was ground in a mortar and then calcined at 800 °C or 850 °C for 3 h to remove the organic residues and obtain the SCF powder, denoted as SCF-P (SCF-P800 or SCF-P850).

Preparation of electrolyte and SCF cathode

$La_{0.9}Sr_{0.1}Ga_{0.8}Mg_{0.2}O_{3-\delta}$ (LSGM) was used as the electrolyte in this study. The LSGM powder was prepared by the solid state reaction method [17]. The LSGM substrate was pressed under 30 MPa into a substrate 1.7 cm in diameter and ~1 mm thick. The powder of SCF-S1250, SCF-S1300, SCF-P850, and SCF-P800 was independently mixed with a terpenol solvent and a certain amount of ethyl cellulose (EC), which acted as a binder. Then, the paste was screen-printed onto the LSGM electrolyte and then sintered at a temperature range of 1,000–1,300 °C for 2 h in air. The electrodes on pellets are tested in air by a three-electrode configuration. The Pt reference electrode was placed on the LSGM electrolyte surface ~1 mm away from the cathode, while the Pt counter electrode applying a Pt paste was coated on another surface of LSGM and then sintering at 800 °C in air for 1 h.

Testing and characterization

The SCF powder prepared by the different chemical routes was characterized by X-ray diffraction, particle analysis, and electrochemical performance measurement. The phase of SCF was examined with a Rigaku D/max-ΠBX-ray diffraction (XRD) using Cu Kα radiation. The particle size distribution of SCF powder was tested with an LS-900 particulate size description analyzer. The surface morphology of the SCF cathode was observed using a scanning electron microscope (SEM, Hitachi S-4700). The electrochemical impedance spectroscopy (EIS) test was conducted at 800 °C with a Princeton Applied PARSTAT 2273 impedance analyzer under the open circuit condition in the frequency range 0.01 to 100 kHz with amplitude of the ac signal 5 mV. The impedance spectra were analyzed in terms of equivalent circuits with the ZSIMWIN software. Cathodic polariza-

tion measurements were obtained at the open circuit voltage in the 0–0.3 V cathodic overpotential range.

Results and discussion

XRD characterization

Figure 1 shows the X-ray diffraction patterns of the SCF powder obtained by different synthesis routes. Figure 1a, b presents the XRD patterns of the SCF powder prepared by the solid state reaction method and Pechini method. It can be seen from the figures that the calcined powder is highly crystalline cubic SCF powder. All major peaks are identifiable to cubic SCF. From the XRD patterns, it is confirmed that the single-phase cubic SCF powders are obtained at a synthesis temperature as low as 800 °C, which
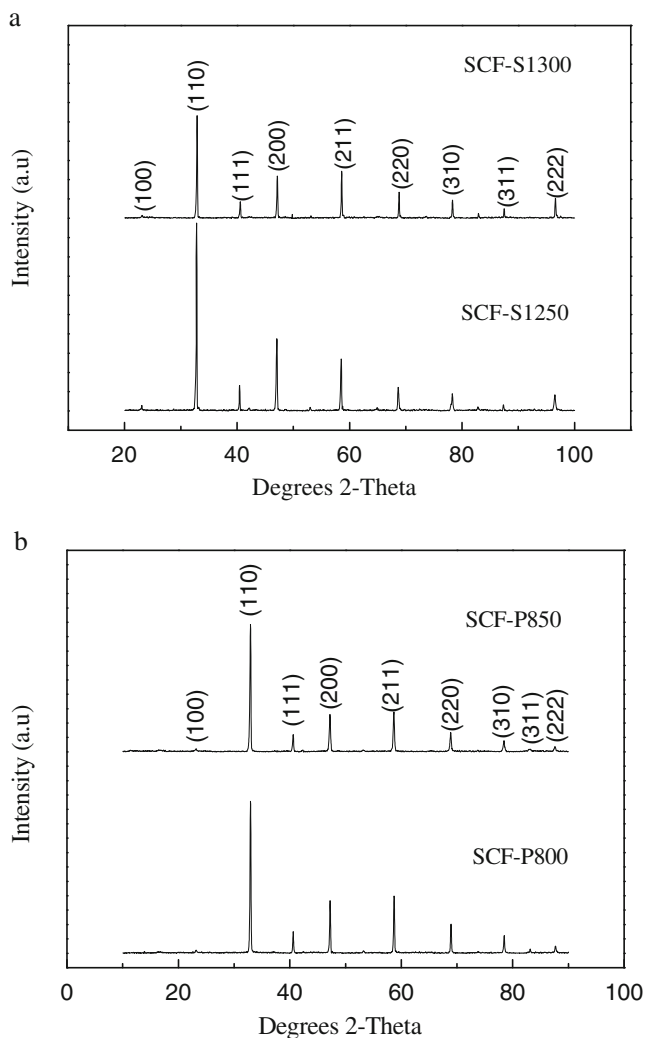
is reduced by 200 °C from 1,000 °C [14]. Also, it is 450 °C lower than that of the solid state reaction method. The solid state oxide reaction method is associated with drawbacks such as diffusional constraints to synthesis results into slow kinetics and high temperatures; however, since the Pechini method involves the mixing of elements at the atomic level, pure SCF phase formation can be accelerated and the synthesis temperature can be lowered [18].

Particle size distribution characterization

Figure 2 shows the particle size distribution of the powder obtained by different synthesis routes. Figure 2a, b presents the particle size distribution of the SCF powder prepared by the solid state reaction method and Pechini method. Table 1 shows the particle size parameter (D_{50}) of the powder. The values of D_{50} indicate that 50% of the particles in the sample are smaller than this diameter. The smaller the D_{50}, the finer the particles [5]. It can be seen from Fig. 2 and Table 1 that with the decrease in the synthesis temperature,
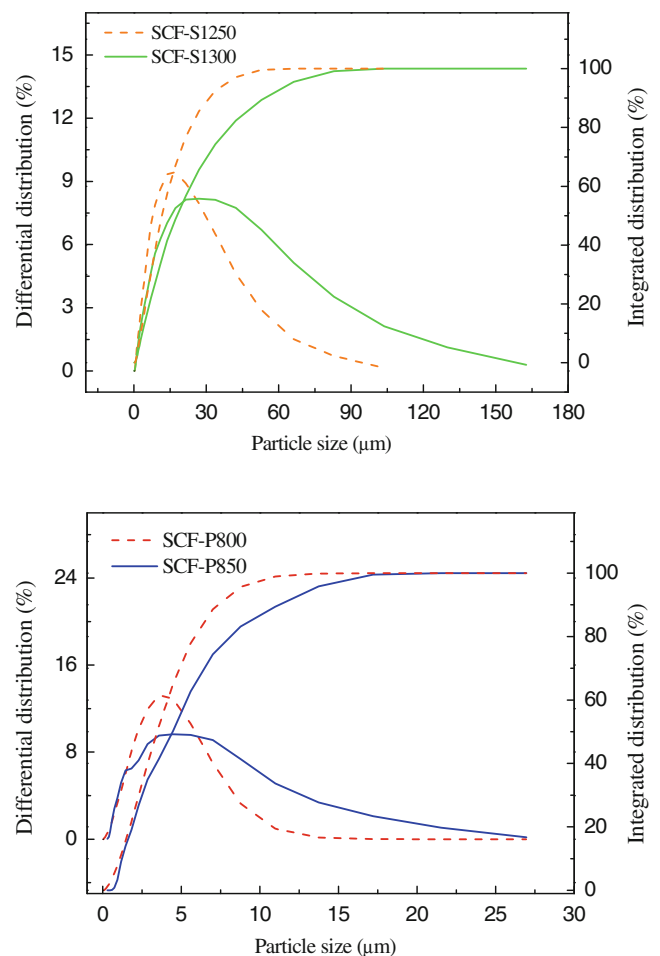

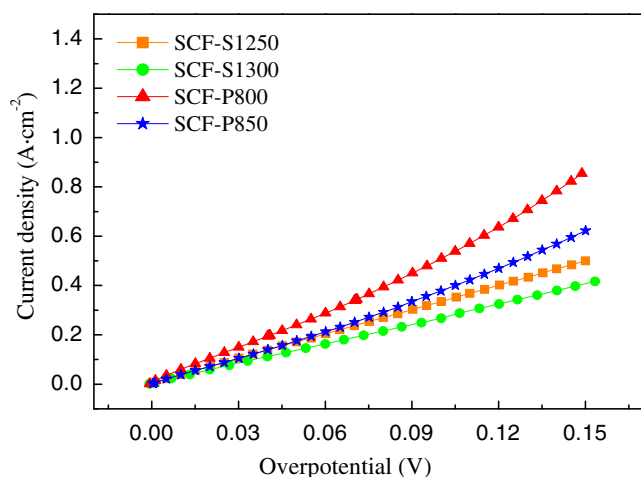**Fig. 1** XRD patterns of **a** SCF-S1300 and SCF-S1250, and **b** SCF-P850 and SCF-P800

Fig. 2 Particle size distribution of **a** SCF-S1300 and SCF-S1250 and **b** SCF-P850 and SCF-P800

Table 1 Particle size parameter (D_{50}) of the SCF powder

Synthesis process	Calcination temperature (°C)	D_{50} (μm)
Solid state reaction process	1,300	17.86
	1,250	11.51
Pechini process	850	3.51
	800	2.72

the SCF particle size decreases in both routes. However, the D_{50} values of SCF-P800 and SCF-P850 are smaller than those of SCF-S1250 and SCF-S1300, especially the D_{50} value of SCF-P800 which is only 2.72 μm, and its particle size distribution was the narrowest in the four kinds of powders. It can be concluded that the Pechini method is beneficial in decreasing the synthesis temperature and particle size of the SCF powders.

Electrochemical performance of SCF cathodes

Figure 3 shows the cathodic polarization curves of the cathodes sintered at 1,000 °C for 2 h, using SCF-S1250, SCF-S1300, SCF-P850, and SCF-P800 as the starting materials. It can be seen from Fig. 3 that the SCF-P cathodes possess better electrochemical performance as compared with the SCF-S cathodes. For the same powder synthesis method, the lower the synthesis temperature, the better the electrochemical performance. This is because the Pechini method is a wet chemical method and has lower synthesis temperature and smaller particle size than the solid state reaction method, so it shows higher electrochemical activity [19].
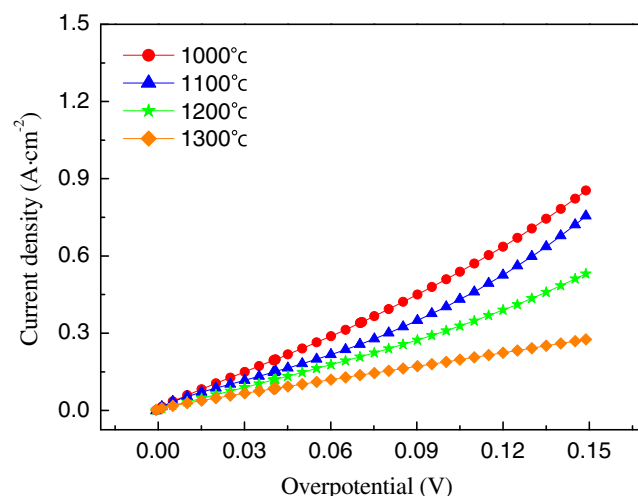
Effect of calcination temperature on the performance of SCF-P cathodes

The influence of CT on the performance of the SCF-P cathodes was investigated in detail. Figure 4 shows the cathodic polarization curves of the SCF-P cathodes sintered at 1,000 °C, 1,100 °C, 1,200 °C, and 1,300 °C for 2 h. It can be seen from Fig. 4 that with the reduction of CT, the electrochemical performance of the SCF-P cathodes is improved gradually. This trend was consistent with previously published studies [14, 20]. The SCF-P cathode sintered at 1,000 °C possesses the best electrochemical performance, and its cathodic overpotential was 0.1 V at the current density of 0.50 A cm^{-2}.

Figure 5 shows the electrochemical impedance spectrums (EIS) and the equivalent circuit of the SCF-P cathodes sintered at various temperatures. The best fitting results for all the impedance spectra were achieved with the equivalent circuit of $LR_{\Omega}(R_1 \Omega_1)(R_2 \Omega_2)$ as shown in Table 2. In contrast, the R_{Ω} was elided in the Nyquist plots, equivalent circuits, and fitting results of SCF-P cathodes. L is the inductance, which is attributed to the platinum current–voltage probes or the high-frequency phase shift of electrochemical equipment; The high-frequency impedance arc, ($R_1 Q_1$), corresponds to charge transfer of oxygen ions on the electrode–electrolyte interfaces. [21, 22]. The low-frequency impedance arc, ($R_2 Q_2$), could be attributed to the adsorption, dissociation, and diffusion of oxygen [22–24]. The equivalent circuit consists of RQ elements. Symbol Q denotes the constant phase element, and their impedances are expressed by the following equation:

$$Z_{CPE} = Y_0^{-1}(jw)^{-n} \tag{1}$$

Fig. 3 Polarization curves of SCF cathodes using various powders as starting materials

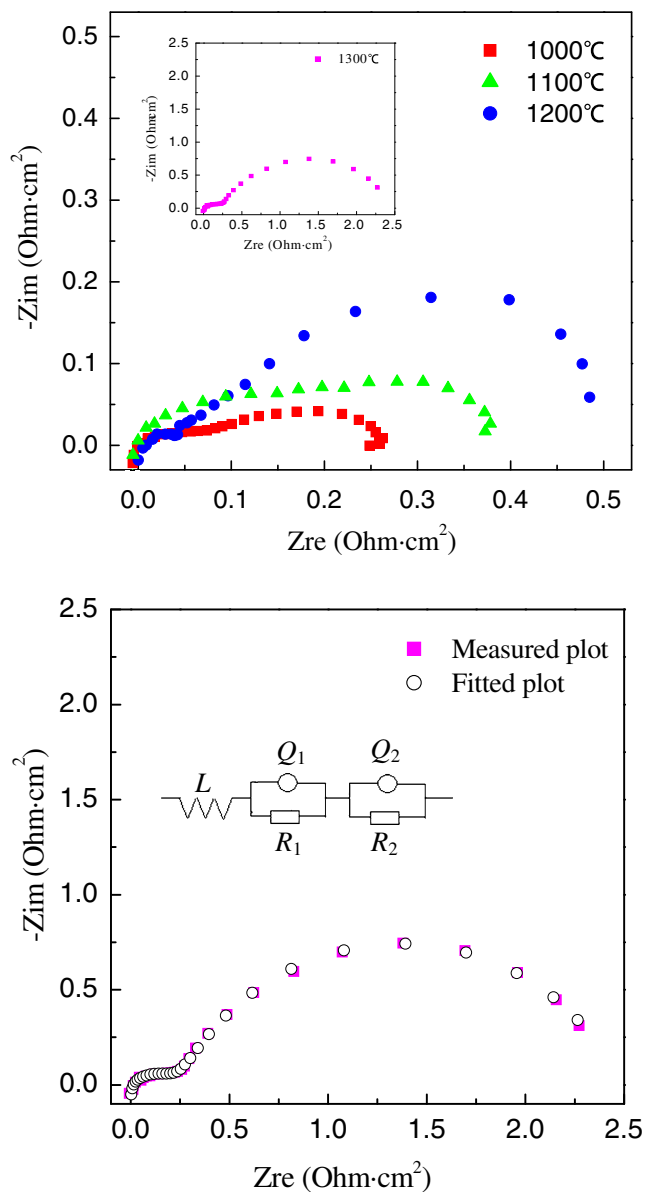**Fig. 4** Polarization curves of SCF cathodes sintered at 1,000 °C, 1,100 °C, 1,200 °C, and 1,300 °C

Fig. 5 Nyquist plots and equivalent circuits of SCF cathodes sintered at different temperatures. **a** Measured Nyquist plots and **b** fitted Nyquist plots

Where Y_0 is a frequency-independent constant, w is the angular frequency ($w = 2\pi f$). j is the square root of -1, and n is an exponential constant. For $n = 1$, 0.5, 0 and -1, Q represents an ideal capacitance, a Warburg impedance, an ideal resistance, and an inductance, respectively [25, 26]. The total polarization resistance of the cathode, R_p, is the sum of R_1 and R_2.

$$R_p = R_1 + R_2 \qquad (2)$$

From Fig. 5 and Table 2, it can be seen that R_p increases gradually with the rise of CT of the SCF-P cathodes. This is consistent with the results of polarization curves for the SCF-P cathodes sintered at various temperatures. The impedance spectra in Fig. 5 comprise two arcs. The low-frequency arc has close relationship with CT, and the high-frequency arc is more or less independent of the CT. This is because R_1 depends not only on the three-phase boundary length (tpbl) but also on the adhesion between cathode and electrolyte. When the CT is low, the adhesion between cathode and electrolyte is poor, but the tpbl is large. On the contrary, for the high CT, the adhesion between cathode and electrolyte is improved, but tpbl is reduced. So, the comprehensive effect of the two factors determines the change of R_1.

It also can be seen from Table 2 that the low-frequency impedances (R_2) are very sensitive to CT, and the change with CT is similar with the total polarization resistance. R_2 increases by nearly 19 times, from 0.11 Ω cm^2 to 2.22 Ω cm^2 with the increase of the cathode CT from 1,000 °C to 1,300 °C. This change may be related to the different microstructures of SCF-P cathodes. Figure 6 shows the surface morphologies of the SCF-P cathodes sintered at different temperatures. It can be seen from Fig. 6 that there are a lot of uniformly distributed pores and effective neck conterminous particles at the surface of SCF-P cathode sintered at 1,000 °C. The number of pores greatly decreased, and particles became large after the cathode was sintered at 1,100 °C. When the CT increased to 1,200 °C or 1,300 °C, the cathodes became relatively dense and represented an oversintered phenomenon that there are a few pores at the surface of cathodes. It is similar to the

Table 2 EIS fitting results of SCF-P cathodes sintered at different temperatures

Temperature (°C)	Q_1		R_1 (Ω cm^2)	Q_2		R_2 (Ω cm^2)	R_p (Ω cm^2)
	$Y_{0,1}$ (Ω^{-1} cm^{-2} s^{-n})	n_1		$Y_{0,2}$ (Ω^{-1} cm^{-2} s^{-n})	n_2		
1,000	1.72	0.74	0.16	0.18	0.56	0.11	0.27
1,100	0.05	0.56	0.26	0.29	0.77	0.16	0.42
1,200	1.60	0.33	0.16	1.51	0.88	0.38	0.54
1,300	0.07	0.47	0.28	0.42	0.75	2.22	2.50

Fig. 6 Surface SEM images of SCF-P cathodes sintered at different temperatures. **a** 1,000 °C, **b** 1,100 °C, **c** 1,200 °C, and **d** 1,300 °C
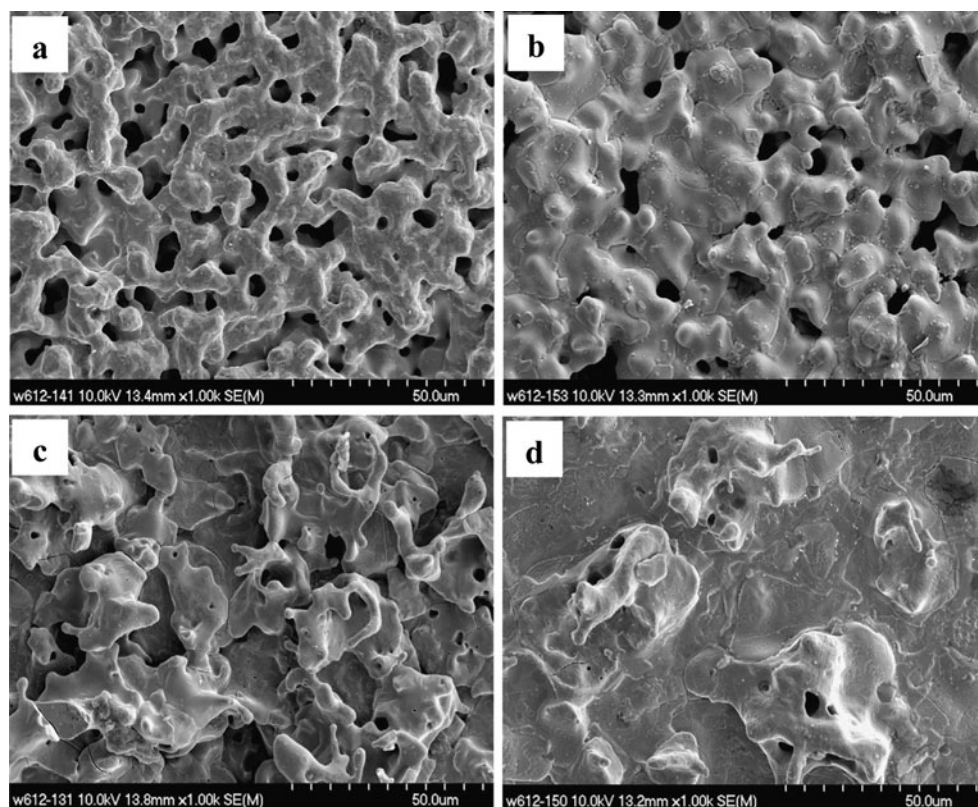
sintering behavior of $La_{0.6}Sr_{0.4}Co_{0.2}Fe_{0.8}O_3$ or $La_{0.8}Sr_{0.2}Co_{0.2}Fe_{0.8}O_3$, in which relative density could reach 92% at 1,200 °C [27, 28]. It is known that Co-based perovskite oxides have high sintering characteristics. So, $SrCo_{0.8}Fe_{0.2}O_{3-\delta}$ with a larger amount of Co prepared above 1,100 °C possesses a high relative density and a low porosity. Thus, the low porosity would increase the resistance of oxygen adsorption, dissociation, and diffusion in the cathode and results in the rise of the low-frequency impedances (R_2). So, with the decrease of CT, the porosity of cathodes increases and the R_2 decreases accordingly.

When CT is above 1,150 °C, the low-frequency impedance is dominant, and the adsorption, dissociation, and diffusion of oxygen is the rate-determining step (RDS). However, for CT under 1,150 °C, R_1 is larger than R_2, but the gap between R_1 and R_2 was not large enough to determine the RDS. So, the charge-transfer process, together with the adsorption, dissociation, and diffusion of oxygen, has a strong influence on the whole reaction process. It is different with the point that the dioxygen dissociation on the gas–solid surface is usually the only rate-limiting step of an MIEC electrode [15, 16]. One effective means to further decrease the charge-transfer resistance is adding an ionically conducting second phase, such as LSGM and doped-CeO_2, which results in increasing the tpbl and suppressing the growth of SCF particles. Our experiments show that adding $La_{0.45}Ce_{0.55}O_{2-\delta}$ to $SrCo_{0.8}Fe_{0.2}O_{3-\delta}$ cathodes can improve the electrochemical perfor-

mance of cathodes, and this portion of work would be published elsewhere.

For these cathodes, the total polarization resistance reduces gradually with the decrease of CT. When the cathode was calcined at 1,000 °C, R_p reached the minimum value of 0.27 Ωcm^2. Further reduction in firing temperature would be beneficial to the enlargement of tpbl and the porosity. But the tight adhesion between cathode and electrolyte would be reduced under the too low CT. In this study, the SCF-P cathode sintered below 1,000 °C may be broken off from
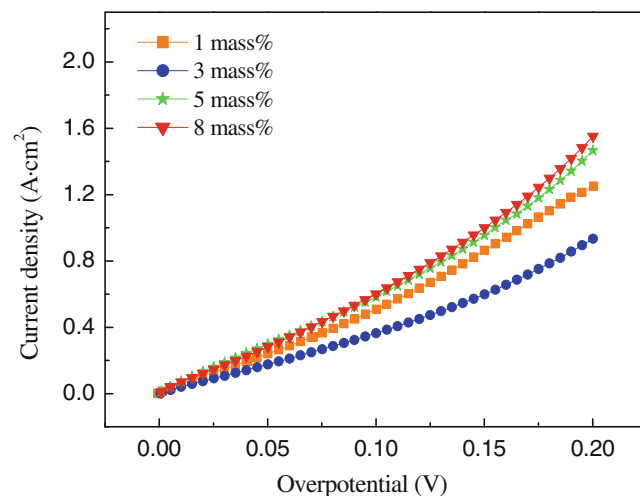

Fig. 7 Influence of amount of EC on the electrochemical performance of SCF cathodes

LSGM electrolyte. So, 1,000 °C was the optimum CT. If the surface of electrolyte was made coarse before the cathode was screen-printed, the adhesion between cathode and electrolyte would be strengthened, and the tpbl should be enlarged. Thus, the optimum CT may be further reduced, and the electrochemical performance also may be improved.

Influence of binder amounts on the performance of SCF-P cathodes

The influence of binder (EC) amounts on the performance of the SCF-P cathodes was studied. Figure 7 shows the cathodic polarization curves of the SCF-P cathodes with different binder contents (1 mass%, 3 mass%, 5 mass%, and 8 mass%). It can be seen from Fig. 7 that with the increase of binder content, the electrochemical performance of SCF-P cathodes is improved gradually, except that of 3 mass%. The SCF-P cathode with 8 mass% binder content possesses the best electrochemical performance, and its cathodic overpotential is 0.1 V at the current density of 0.61 A·cm^{-2}. On one hand, it may be related to the enhancement of the adhesion between cathode and electrolyte by introducing the binder into the cathode paste. On the other hand, EC may also play a role on pore forming. This needs further study. As for the precise influence mechanisms, further work is necessary.

Conclusions

SrCo$_{0.8}$Fe$_{0.2}$O$_{3-\delta}$ was successfully synthesized by the solid state reaction method and Pechini method. Single-phase cubic SCF powder was obtained by the Pechini method at synthesis temperature as low as 800 °C, which was reduced by 200 °C from 1,000 °C. Also, it was 450 °C lower than that of solid state reaction method. With the decrease of synthesis temperature, the SCF particle size decreases, and its electrochemical performance increases in both routes. The SCF-P has a smaller particle and possesses better electrochemical performance as compared with the SCF-S cathodes. The reason is that the Pechini method involves the mixing of elements at atomic level, so pure SCF phase formation can be accelerated and showed high electrocatalytic activity. Calcination temperature has influence on the tpbl, porosity of cathode, and the adhesion between cathode and electrolyte. The R_p and R_2 decrease gradually with the reduction of calcination temperature for SCF-P cathodes. SCF-P cathode sintered at 1,000 °C possesses the biggest porosity and the best electrochemical performance, and the rate-limiting step was charge-transfer process together with the adsorption, dissociation, and diffusion of oxygen. With the increase of EC content, the electrochemical performance of SCF-P cathodes was improved gradually.

SCF-P cathode with 8 mass% EC content reached the lowest cathodic overpotential of 0.1 V at the current density of 0.61 Acm^{-2}. The thermal expansion coefficient of SCF cathode material is 24×10^{-6} K^{-1} and much larger than that of the LSGM electrolyte, so further studies of the long-term stability of SCF cathode are necessary.

References

1. Murray EP, Tsai T, Barnett SA (1999) Nature 400:649
2. Flytzani-Stephanopoulos M, Sakbodin M, Wang Z (2006) Science 312:1508
3. Park EW, Moon H, Park MS, Hyun SH (2009) Int J Hydrocarb Eng 34:5537
4. Steele BCH (2001) Nature 414:345
5. Zhu XD, Sun KN, Le SR, Zhang NQ, Fu Q, Chen XB, Yuan YX (2008) Electrochim Acta 54:862
6. Hibino T, Hashimoto A, Inoue T, Tokuno JI, Yoshida SI, Sano M (2000) Science 288:2033
7. Huang B, Wang SR, Liu RZ, Ye XF, Nie HW, Sun XF, Wen TL (2007) J Power Sources 167:39
8. Ishihara T, Matsuda H, Takita Y (1994) J Am Chem Soc 116:3801
9. Feng M, Goodenough JB (1994) Eur J Solid State Inorg Chem 31:663
10. Takeda Y, Sakaki Y, Ichikawa T, Imanishi N, Yamamoto O, Mori M, Mori N, Abe T (1994) Solid State Ionics 72:257
11. Jiang SP, Love JG (2003) Solid State Ionics 158:45
12. Huang K, Goodenough JB (2001) J Electrochem Soc 148:E203
13. Huang K, Wan J, Goodenough JB (2001) J Mater Sci 36:1093
14. Huang KQ, Wan JH, Goodenough JB (2001) J Electrochem Soc 148:A788
15. Adler SB (1998) Solid State Ionics 111:125
16. Adler SB, Reimer JA (1996) Solid State Ionics 91:175
17. Zhu XD, Zhang NQ, Wu LJ, Sun KN, Yuan YX (2010) J Power Sources 195:7583
18. Gosavi PV, Biniwale RB (2010) Mater Chem Phys 119:324
19. Sasaki K, Wurth JP, Gschwend R, Gödickemeier M, Gauckler LJ (1996) J Electrochem Soc 143:530
20. Jørgensen MJ, Primdahl S, Bagger C, Mogensen M (2001) Solid State Ionics 139:1
21. Baumann FS, Fleig J, Konuma M, Starke U, Habermeier HU, Maier J (2005) J Electrochem Soc 152:A2074
22. Zhu XD, Sun KN, Zhang NQ, Chen XB, Wu LJ, Jia DC (2007) Electrochem Commun 9:431
23. Yang YL, Chen CL, Chen SY, Chu CW, Jacobson AJ (2000) J Electrochem Soc 47:4001
24. Murray PE, Sever MJ, Barnett SA (2002) Solid State Ionics 148:27
25. Kek D, Panjan P, Wanzenberg E, Jamnik J (2001) J Eur Ceram Soc 21:1861
26. Fu CJ, Chan SH, Liu QL, Ge XM, Pasciak G (2010) Int J Hydrocarb Eng 35:301
27. Shao J, Tao YK, Wang JX, Xu C, Wang WG (2009) J Alloys Compd 484:263
28. Leng YJ, Chan SH, Liu QL (2008) Int J Hydrocarb Eng 33:3808